Low Distortion Null-Steering Beamforming with a Cascade of Fiber Bragg Grating Gires-Tournois

M. E. Mousa Pasandi, M. M. Sisto, S. LaRochelle, L. A. Rusch
Centre d'optique, photonique et laser (COPL), Université Laval, Québec, G1K7P4, Canada
larochel@gel.ulaval.ca

Abstract— **We characterize the performance of a FBG-based null-steering beamformer (independent control of amplitude and phase of a multi-element antenna array), via numerical simulations and experimental characterization of achievable EVM for IEEE 802.11a/n signals.**

I. INTRODUCTION

Null-steering beamforming techniques require not only control of phase (as for conventional beamforming), but also independent control of the amplitude [1]. Recently we proposed a novel optical null-steering beamformer [2] based on Gires-Tournois fiber Bragg gratings for radio over fiber (ROF) communication systems with a 5 GHz RF carrier frequency. Figure 1(a) shows the link architecture. Simultaneous and independent control over the amplitude and phase of the signal for each array element gives not only beam steering capability but it also allows better interferer nulling and reduction of sidelobe level. Furthermore, the multi-peak spectral response of the device makes it compatible with wavelength multiplexed antenna remoting links with regular double sideband (DSB) modulation systems. FBG-based devices, however, are known to present an imperfect spectral response that introduces some level of amplitude and phase distortion. Although the impact of these ripples on digital communication systems has been widely studied, little has been reported on grating penalty in ROF systems. On the other hand, this system affects the relative phase of the optical spectrum components and the study of its impact on a complex signal like IEEE 802.11a/n is indispensable to prove the reliability of this null-steering beamformer in ROF applications for indoor communication. In this paper, we focus on one channel and characterize the phase response of this tunable FBG-based null-steering beamformer by performing error-vector-magnitude (EVM) measurements and simulations. Note that while this device is not "true time delay" (its bandwidth is limited by the maximum allowable beam squint), beam squint is not an issue for indoor networks employing IEEE 802.11a/g/n with 40 MHz bandwidth or less.

II. GIRES-TOURNOIS NULL-STEERING BEAMFORMER ARCHITECTURE

The Gires-Tournois null-steering beamformer (GT-BF) is composed of a cascade of two Gires-Tournois fiber Bragg grating filters (GT-FBG), with 25 GHz free-spectral-range, that are fabricated by superimposing two chirped gratings with a 4 mm longitudinal offset. The two GT-FBGs of the cascade have opposite chirp. A schematic of the delay response of each GT-FBG over one FSR is shown in Figure 1(b): the FBG chirp causes a linear increase (decrease) in the group delay response that adds up with a delay peak at the cavity resonance frequency. The total group delay response is shown in Figure 1(c): flat over the FSR except for

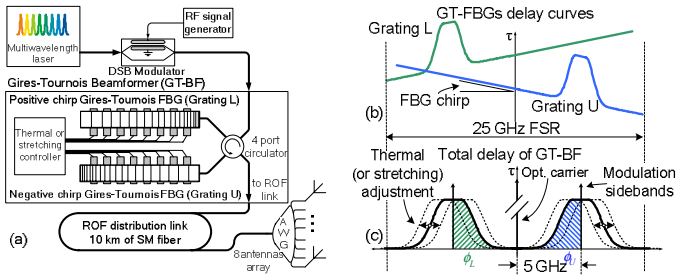

Figure 1: ROF link architecture (a), group delay responses of GT-FBGs in each FSR (b), and the total group delay response of GT-BF in each FSR (c).

the two peaks. Considering fiber dispersion, the detected RF voltage signal feeding an antenna element at ω_{RF} is proportional to:

$$V_{RF} \propto \cos\left(\phi_L - \phi_U + \frac{L_f D}{4\pi c}\lambda_0^2\omega_{RF}^2\right)\cdot\cos\left(\omega_{RF}t + \phi_L + \phi_U\right), \quad (1)$$

where D is the dispersion, L the fiber length, c the speed of light and λ_0 the optical carrier wavelength. According the definition of filter phase response, ϕ_U and ϕ_L are:

$$\phi_L = \frac{1}{2}\int_{-\omega_{RF}}^{0}\tau(\omega)\,d\omega \qquad \phi_U = \frac{1}{2}\int_{0}^{\omega_{RF}}\tau(\omega)\,d\omega \quad (2)$$

where $\tau(\omega)$ is the GT-BF group delay response. Shaded areas in Figure 1(c) are corresponded to ϕ_U and ϕ_L. By applying temperature or strain to the GT-FBGs, the delay peaks in Figure 1(c) can be shifted independently in order to increase or decrease the value of the integrals in (2). According to (1), we have "$\phi_L+\phi_U$ term" as the signal phase and "ϕ_L-ϕ_U term" in the signal amplitude. Therefore by independent adjusting of ϕ_U and ϕ_L, independent control of signal phase and amplitude is possible. Note also that by a wise selection of the "ϕ_L-ϕ_U term", GT-BF can compensate for chromatic dispersion of the ROF link. Furthermore, due to the spectrally periodic phase response of the GT-FBGs, the signal from a multiwavelength source can be processed by a single null-steering beamformer and then demultiplexed to feed an antenna array. Because of the underlying chirp of the fiber grating structures that spatially separates the resonating fields at each wavelength along the fiber axis, independent tuning of each signal can be obtained by the use of a segmented heater as represented in Figure 1 [3].

III. EXPERIMENTAL VERIFICATION OF NULL-STEERING BEAMFORMER IMPACT ON IEEE 802.11A/N SIGNALS

The IEEE 802.11a/g/n protocols are based on OFDM modulation with RF carrier frequency of 5 GHz, with 20 MHz or 40 MHz bandwidth. In these standards, multi-level quadrature amplitude modulation (QAM) is used for high speed data transmission: the 802.11a maximum transmission rate is achieved using 64-QAM that is very sensitive to link

noise and intermodulation distortion. Furthermore, the OFDM signals are characterized by a high peak-to-average-power ratio (PAPR) which increases the signal sensitivity to distortion. Narrowband signals such as IEEE 802.11a/g/n are mostly affected by the third-order intermodulation distortion (ID3), because even-order distortion terms can be filtered in the RF domain. In many ROF links, the optical modulator is the main source of ID3.

In order to experimentally verify the performance of GT-BF, the ROF link consisted of a DFB laser, a Mach-Zehnder modulator (MZ), the GT-BF and an amplified photodetector. The RF input to the modulator was provided by a vector signal generator (VSG), and the received signal was fed to a vector signal analyzer (VSA). We transmitted 64-QAM IEEE 802.11a signals at 5 GHz over the ROF link: the signals were composed of frames with a synchronization symbol, a channel-response training symbol, and a payload of 16 OFDM-symbols. After detection, the 64-QAM symbols are extracted to measure the EVM, a common performance metric of OFDM signals. The electrical back-to-back EVM measurement, with the VSG directly connected to the VSA, was -48.7 dB. EVM measurement at the MZ output was -37.2 dB. This EVM degradation is expected and arises from MZ third-order distortion. The MZ modulator bias was set at the quadrature point.

The position of the GT-BF delay peaks can be changed independently by using their respective temperature controllers to achieve the desired value for amplitude and phase according to (1) and (2). We generated and transmitted several different data frames for several positions of the delay peaks, and measured the received phase and average EVM. The results are presented as a function of the frequency shift of the left and right delay peaks relative to the center of the lower and upper modulation sidebands respectively. Figure 2(a) and 2(b) presents the phase simulation and measurement results, respectively. For beamforming applications, a particular region of interest is around the diagonal (in the rectangular zone), where a 1.5π phase shift can be obtained by symmetrical displacement of group delay peaks.

The simulated and measured EVM maps are shown in Figures 3(a) and 3(b), respectively. The simulations were done with the ideal GT-BF response used as design goal of the experimental device. Strong attenuation of the signal amplitude eventually degrades the EVM as is apparent in the lobes of Figure 3(b). However in the rectangular zone of interest the EVM is less than -38 dB which complies with the protocol acceptance threshold of -25 dB and common commercial values of -35 dB. The simulated and measured EVM on the diagonal, across the rectangular zone, has been drawn in Figure 4. The measured EVM on the diagonal has a floor not found in simulations. This is probably due to additive noise and distortion introduced by the EDFA and RF amplifier. Nonetheless, the EVM measured after the GT-BF is better than the EVM measured after the MZ modulator (solid straight line in Figure 4), indicating that some compensation of the nonlinearity takes place. This phenomenon has been reported before, for example in [4] it was shown that by wisely manipulating the optical spectrum, some of the ID3 generated by the modulator can be suppressed. For example, fiber dispersion can change the relative phase of different components of the propagating spectrum such that the received ID3 at the fiber end may be less than what is measured at the modulator output. In the GT-BF case, we believe this to result from the different amounts of group delay in GT-BF experienced by the various ID3 components, leading to partial cancellation of the nonlinear terms.

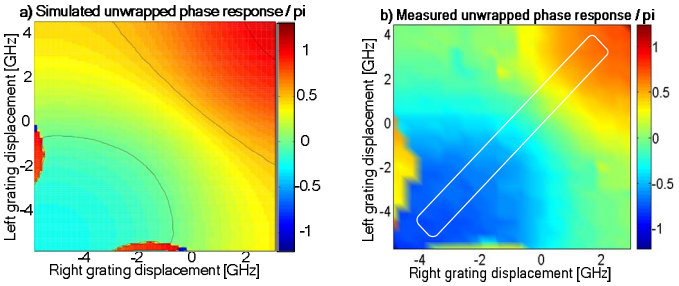

Figure 2: Simulated (a) and measured (b) unwrapped phase response of the GT-BF as a function of frequency shift of the delay peaks.

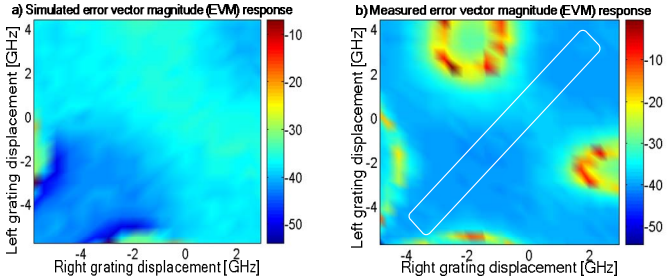

Figure 3: Simulated (a) and measured (b) EVM after the GT-BF as a function of frequency shift of the delay peaks.

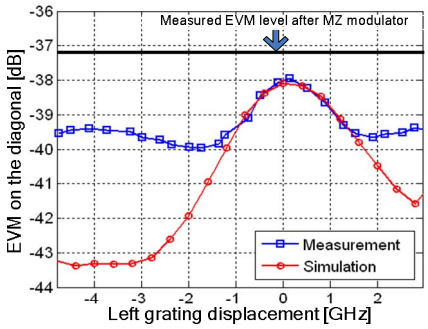

Figure 4: Simulated EVM and measured EVM on the diagonal.

IV. Conclusion

We demonstrated a tunable multi-channel FBG-based Gires-Tournois null-steering beamformer that does not distort IEEE 802.11a/n signals over a range of 1.5π phase shift. The null-steering beamformer also compensates some of the nonlinearities induced by the EO modulator. In future work, improved performance will be achieved with a three-cavity GT-FBGs design. Numerical simulations show that this device will allow 2π phase shifts and amplitude control of RF signals [2]. We believe that this compact and easily reconfigurable device is well-suited for WDM feeding of antenna arrays.

References

[1] Godara, L. C., "Applications of antenna arrays to mobile communications. I," in *Proc. of the IEEE*, vol. 85, pp. 1031-1060, 1997.

[2] Sisto M. M. et al, "Optical Phase and Amplitude Control for Beamforming with Multiwavelength Gires-Tournois Bragg Grating Cavities," in *Proc. of 4th IASTED Int. Conf. on. Antennas, Radar, and Wave Propagation (ARP)*, Montreal, Quebec, Canada, May. 2007.

[3] Doucet S. et al, "Multi-channel tunable chromatic dispersion compensator and profiler," in 31st European Conference on Optical Communication, vol. 3, pp. 421-422, Glasgow, UK, 2005.

[4] Tae-Sik C. et al, "Effect of Third-Order Intermodulation on Radio-Over-Fiber Systems by a Dual-Electrode Mach–Zehnder Modulator With ODSB and OSSB Signals," *IEEE J. Lightwave Technol.*, vol. 24, pp 2052-2058, May. 2006.